博 士 論 文

Characterization and antibacterial assessments of Ag nanoclusters / rose bengal nanocomposite for antimicrobial photodynamic therapy

（抗菌的光線力学療法に向けた銀ナノクラスター/
ローズベンガル複合体の特性並びに抗菌性評価）

平成 31 年 3 月申請

北海道大学
大学院歯学研究科口腔医学専攻

蔀　佳　奈　子

Title

Characterization and antibacterial assessments of Ag nanoclusters / rose bengal nanocomposite for antimicrobial photodynamic therapy

Kanako SHITOMI, Hirofumi MIYAJI, and Tsutomu SUGAYA

Affiliation

Department of Periodontology and Endodontology, Faculty of Dental Medicine, Hokkaido University, N13 W7, kita-ku, Sapporo, 060-8586, Japan

Corresponding author

Kanako SHITOMI

E-mail: shitomi@den.hokudai.ac.jp

Key words

Aggregatibacter actinomycetemcomitans, Photosensitizer, *Porphyromonas gingivalis*, Singlet oxygen, *Streptococcus mutans*

Running title

Photodynamic effects of AgNCs/RB

Number of pages, tables and figures

27 pages, 4 figures

Abstract

Ag nanoclusters (AgNCs) / rose bengal (RB) nanocomposite (AgNCs/RB) as a novel photosensitizer was created for antibacterial photodynamic therapy (a-PDT). We proposed double antibacterial effects of photoexcited AgNCs/RB; (1) singlet oxygen ($^1O_2$) generated by irradiated RB and (2) Ag^+ ion released by AgNCs oxidized by $^1O_2$. In present study, the antimicrobial and the cytotoxic effects of AgNCs/RB were evaluated.

$^1O_2$ generation, zeta potential and Ag^+ release of AgNCs/RB was characterized. Subsequently, the antimicrobial effect of AgNCs/RB irradiated by white light-emitting diode (LED) was evaluated using oral bacterial cells; *Streptococcus mutans, Porphyromonas gingivalis and Aggregatibacter actinomycetemcomitans.* In addition, cytotoxicity of AgNCs/RB on NIH3T3 mammalian cells was investigated.

The binding of AgNCs and RB, $^1O_2$ generation and Ag^+ ion release of photoexcited AgNCs/RB were estimated. AgNCs/RB irradiated by white LED (60 sec) showed significantly inhibited the growth of oral bacteria when compared to AgNCs or RB. In addition, photoexcited AgNCs/RB did not negatively affect the adhesion, spreading and proliferation of mammalian cells, even at concentrations that showed antibacterial activity.

In conclusion, AgNCs/RB irradiated by white LED showed great antimicrobial effects via $^1O_2$ generation and Ag^+ ion releasing and low cytotoxic properties to be provided for dental a-PDT.

1. Introduction

Antimicrobial photodynamic therapy (a-PDT) has a potential of bacterial sterilization via generation of active oxygen species using light-irradiated photosensitizer. The a-PDT application has recently received broad attention as effective dental treatment, such as dental caries, periodontitis, peri-implantitis and endodontic therapy[1-3]. Several organic dye photosensitizers, including rose bengal (RB)[4], indocyanine green[5], toluidine blue[6] and methylene blue[4], have been clinically employed for a-PDT. Compared to antimicrobial drugs, dye system of a-PDT has advantages regarding allergy to drugs, antibiotic-resistant bacteria[7] and biofilm destruction[8], however, conventional photosensitizers have some problems for clinical use. Since $^1O_2$ generated by conventional photosensitizer has a short half-time of about 200 ns[9], antibacterial effect will be soon disappeared after light-out. The low photo-stability of organic dye also decreases the antibacterial ability[10]. In addition, the oxygen-concentration dependency of PDT would reduce the PDT efficiency in the region of low oxygen concentration around anaerobic oral/ dental infection. Hence, the creation of novel photosensitizer is required for the enhancement of the antibacterial effect of a-PDT.

Precious and heavy metal; Ag, have been previously known to possess antimicrobial properties[11]. Many researchers have attempted to apply the synthesized Ag substrates for medical applications[12]. Castillo et al.[13] reported that application of $Ag(NH_3)_2F$ to the dental caries modified tooth substrate via deposition of Ag and inhibited the bacterial cell attachment and caries progression. In addition, medical devices penetrating skin, such as, dental implant[12,14] and catheters[15], was mixed with Ag substrate to obtain the antibacterial effects via Ag^+ ion release from its surface. Recently, there has been a growing interest in water-soluble Ag nanoclusters (AgNCs) as antibacterial agents because of their ultrasmall sizes (<2 nm) and high antibacterial activity[11,16]. We previously succeeded to synthesis of antibacterial AgNCs with tetraoctylammonium and showed its stability[17]. As far as we know, however, there have been few reports about the application of AgNCs for effective dental treatments.

In present study, we first created the nanocomposite of AgNCs with rose bengal (AgNCs/RB) to show highly efficient antibacterial activity by the light-induced two actions: the generation of singlet oxygen ($^1O_2$) by RB and releasing of Ag^+ ion from AgNCs. The antibacterial activity of AgNCs/RB against oral bacterial cells (*Streptococcus mutans*, *Aggregatibacter actinomycetemcomitans*, and *Porphyromonas gingivalis*) was evaluated. Furthermore, cytotoxicity of AgNCs/RB was assessed using

mammalian fibroblastic NIH3T3 cells. To solve the disadvantages of organic dye photosensitizers, we speculated that the nanocomposite of RB and AgNCs exerted great photodynamic effects for antibacterial therapy. In addition, when AgNCs are configured close to RB with nanoscale, $^1O_2$ generated by RB will oxidize AgNCs to release Ag^+ ions. Thus, we propose integrated double antibacterial strategies for dental a-PDT via AgNCs/RB nanocomposite; bacterial cells are damaged under a white light-emitting diode LED irradiation by (1) $^1O_2$ generated by photoexcited RB and (2) Ag^+ ion released by AgNCs oxidized by RB.

2. Materials and methods

All chemicals were used as received without further purification. Glutathione (reduced form, GSH, 98%), methanol (99.7%), D_2O (99.9%) and silver nitrate ($AgNO_3$, 99.9%) were purchased from FUJIFILM Wako Pure Chemical Corporation Ltd. (Osaka, Japan). Sodium borohydride ($NaBH_4$, 99.99%) was purchased from Sigma-Aldrich (St. Louis, MO).

The bacterial strains used in this study were *Streptococcus mutans* ATCC 35668, *Aggregatibacter actinomycetemcomitans* ATCC 29522, *Porphyromonas gingivalis*

ATCC 33277. These strains were kept frozen until analysis. Bacterial stocks were incubated in brain heart infusion (BHI) broth (Pearlcore®, Eiken Chemical, Co., Ltd., Tokyo, Japan) supplemented with 0.1% antibiotics (gramicidin D and bacitracin; FUJIFILM Wako Pure Chemical Corporation Ltd.) and 1% sucrose (FUJIFILM Wako Pure Chemical Corporation Ltd.) for *S. mutans*; 1% yeast extract (FUJIFILM Wako Pure Chemical Corporation Ltd.) for *A. actinomycetemcomitans*; and 0.5% yeast extract, 0.0005% hemin and 0.0001% menadione for *P. gingivalis*.

2.1 Synthesis of AgNCs/RB

AgNCs (i.e. $Ag_{32}(SG)_{19}$) were obtained by the ultra violet (UV) photo-mediated size-focusing synthesis according to the literature[18]. This photo-mediated size-focusing synthesis comprises a two-step protocol: (i) the reduction of Ag ions by $NaBH_4$ to form polydisperse AgNCs intermediates and (ii) the subsequent photo-mediated size-focusing of these intermediates under 365 nm UV irradiation, producing monodisperse $Ag_{32}(SG)_{19}$. AgNCs/RB nanocomposite was prepared through the interaction between AgNCs and RB. A 1 mM RB solution and a 1 mM AgNCs solution were prepared as stock solutions. The RB solution was mixed with the AgNCs solution in mole ratio of 1:0.3 (AgNCs:RB). The resultant solution was stirred at 200 rpm for 2 hr using a

magnetic stirrer. After that, the solution was purified with a centrifugal ultrafiltration tube (Amicon® Ultra-Centrifugal Filters, 3 KD; Merck, Darmstadt, Germany) to discard the free RB. After centrifuged ultrafiltration, the filtrate solution did not contain RB, indicating the binding of RB into the AgNCs.

2.2. Characterization

UV-vis (absorption) spectra were recorded using a UV-vis-NIR spectrophotometer (V-670, JASCO, Tokyo, Japan) and a fluorometer (FP-6300, JASCO, Tokyo, Japan), respectively. Measurements of zeta potential were performed on a Malvern Zetasizer Nano ZS instrument (Malvern Instruments Ltd. Worcestershire, UK) equipped with a HeNe laser operating at 632.8 nm. Inductively coupled plasma mass spectrometry (ICP-MS, Agilent Technologies, 7900, Tokyo, Japan) was utilized to determine the concentration of Ag in aqueous sample solutions.

2.3 Detection of $^1O_2$ generation by AgNCs/RB

$^1O_2$ generation by photoexcited AgNCs/RB under white LED light irradiation (a wavelength of 420-750 nm, 80 mW/cm^2, SPF-D2, Shodensha, Osaka, Japan) was evaluated using methotrexate (MTX, FUJIFILM Wako Pure Chemical Corporation

Ltd.) as a chemical probe of $^1O_2$. MTX can selectively react with $^1O_2$, resulting in increased fluorescence intensity[19]. The concentration of the AgNCs was adjusted to be equal absorbance (ca. 0.1) at 532 nm. A 10 mM stock solution of MTX in *N,N*-dimethylformamide was prepared and then added to a 2 mL aqueous solution (D_2O) to yield a final concentration of MTX of 20 mM. The solutions were then irradiated with a white LED light. The fluorescence spectra were recorded using a spectrofluorometer.

2.4 Antimicrobial effects of AgNCs/RB

AgNCs/RB (final concentration: 0, 0.01, 0.1, 1 and 10 μg/mL) were dissolved in the suspension of *S. mutans* (final concentration: 5.5×10^6 colony-forming unit [CFU]/mL), *A. actinomycetemcomitans* (final concentration: 1.1×10^6 CFU/mL) and *P. gingivalis* (final concentration: 3.7×10^7 CFU/mL). After irradiation by white LED light for 1 min, suspension was incubated for 24 hr under anaerobic incubation at 37°C. After that, the turbidity of each suspension was measured using a turbidimeter (CO7500 Colourwave, Funakoshi Co. Ltd., Tokyo, Japan) at 590 nm.

To observe the morphology of *S. mutans,* suspension of *S. mutans* added with AgNCs/RB (0 and 10 μg/mL) was irradiated by white LED light for 1 min and

incubated for 24 hr. The samples were fixed in 2.5% glutaraldehyde in 0.1 M sodium cacodylate buffer (pH 7.4) and dehydrated in ethanol to analyze using scanning electron microscopy (SEM; S-4000, Hitachi Ltd., Tokyo, Japan) at an accelerating voltage of 10 kV after Pt-Pd coating. In addition, some samples were stained by the LIVE/DEAD BacLight Bacterial Viability Kit (Thermo Fisher Scientific, Waltham, MA) and observed using fluorescence microscopy (Biorezo BZ-9000, Keyence Corporation, Osaka, Japan).

To compare the antimicrobial effect, AgNCs (10 μg/mL), AgNCs/RB (10.35 μg/mL) and RB (0.35 μg/mL) were added to suspension of *S. mutans* and *A. actinomycetemcomitans* and received white LED light irradiation (0 and 1 min). After 24 hr culture, turbidity of suspension was measured. In addition, *S. mutans* suspensions including AgNCs/RB (1 μg/mL) received the irradiation with 0, 30, 60, 90 or 120 sec, to assess the time-dependent a-PDT effect. After incubation for 24 hr, the bacterial turbidity was measured. To investigate the influence of Ag^+ ion release on antibacterial activity, BHI medium contained 10 μg/mL AgNCs/RB was photoexcited with LED irradiation (1 min). After waiting 10, 60 and 900 sec, *S. mutans* suspension was mixed into medium. The turbidity of the 24 hr cultured suspension was measured.

2.5 Cytotoxic evaluation of AgNCs/RB

To compare the cytotoxicity, AgNCs (10 μg/mL), AgNCs/RB (10.35 μg/mL) and RB (0.35 μg/mL) were added to suspension of 1×10^4 mouse osteoblastic NIH3T3 cells (RIKEN BioResource Center, Tsukuba, Japan) and received white LED light irradiation (0 and 1 min). Cells culture was performed in 96-well plates using culture medium (minimum essential medium alpha, GlutaMAX-I, Thermo Fisher Scientific) supplemented with 10% fetal bovine serum (Qualified FBS, Thermo Fisher Scientific) and 1% antibiotics (Penicillin-Streptomycin, Thermo Fisher Scientific) at 37°C with 5% CO_2. The cytotoxicity after 24 hr incubation was determined using the water-soluble tetrazolium salt (WST)-8 assay (Cell Counting Kit-8, Dojindo Laboratories, Mashiki, Japan) and lactate dehydrogenase (LDH) assay (Cytotoxicity LDH Assay Kit-WST, Dojindo Laboratories). The absorbance at 450 nm (WST-8) and 490 nm (LDH) was measured on a microplate reader (ETY-300, Toyo Sokki, Yokohama, Japan).

In addition, vinculin-F-actin double staining of incubated cells was performed. The cultured cells were permeabilized with 0.5% Triton X-100 for 10 min and then, cells were incubated for 30 min with bovine serum albumin (BSA) (7.5 w/v% Albumin Dulbecco's-PBS(-)Solution, from Bovine Serum, FUJIFILM Wako Pure Chemical Corporation Ltd.) as blocking buffer. A staining solution was prepared by dissolving

4μL of 0.5 mg/mL anti-vinculin monoclonal antibody (Anti-Vinculin Alexa Fluor 488, eBioscience, San Diego, CA), 3 μL of 20 μg/mL phalloidin (Acti-stain 555 fluorescent Phalloidin, Cytoskeleton Inc., Denver, CO) and 3 μL of 1 mg/mL 4',6-diamidino-2-phenylindole solution (Dojindo Laboratories) in 500 μL of BSA. The mixture was kept shaking for 1 hr at 37°C. After 24 hr at 4°C, the sample was washed and observed using fluorescence microscopy. Some samples were stained using the LIVE/DEAD Viability/Cytotoxicity Kit for mammalian cells (Thermo Fisher Scientific), Stained samples were observed using fluorescence microscopy.

2.6 Statistical analysis

Statistical analyses were performed by Scheffé and Games Howell tests. *P* values <0.05 were considered statistically significant. All statistical procedures were performed using a software package (SPSS 11.0, IBM Corporation, Armonk, NY).

3 Result

3.1 Synthesis and characterization of AgNCs/RB

Fig. 1A shows the UV-vis spectra of AgNCs, RB, and the AgNCs/RB. The AgNCs show the absorption peak at 485 nm, which is consistent with that of $Ag_{32}(SG)_{19}$[18]. Upon conjugation of RB with the AgNCs, the RB absorption is observed at around 550 nm in the AgNCs/RB nanocomposite. This indicates the binding of RB into the AgNCs. The binding was also supported by the decrease of the ξ value from -27 mV (AgNCs) to -51mV (AgNCs/RB) due to the negatively charged RB (Fig. 1B).

3.2 Detection of $^1O_2$ generation by AgNCs/RB

The $^1O_2$ generation by photo-excited AgNCs/RB was evaluated with a chemical trap $^1O_2$ probe, MTX. The AgNCs/RB has broad absorbance in the UV-vis range of less than 700 nm, and hence a white LED was chosen as an effective photo-excitation source for the nanocomposite. The fluorescence spectra of MTX in the presence of the AgNCs/RB in D_2O were obtained. In the dark, there was no change in the fluorescence spectra of MTX. Under white LED irradiation for 10 min., the fluorescence intensities at 466 nm increased over time due to the oxidation of MTX by $^1O_2$ generated by the nanocomposite (Fig. 1C)[20].

Fig. 1D shows the UV-vis spectra of AgNCs/RB before and after the white LED irradiation for 20 min. It is clear from the absorbance decrease that the LED irradiation

caused the degradation of both RB and the AgNCs in the nanocomposite: the absorbance decreases at 550 nm for RB and at 440 nm for AgNCs. The ratio of absorbance decrement at 440 nm is more enhanced in the AgNCs/RB (~5%) than that of AgNCs alone (~1%), as shown in Fig 1E. This suggests the enhanced photo-induced degradation of AgNCs by the conjugate of RB. The AgNCs conjugated to RB will be oxidized by the $^1O_2$, resulting in the release of Ag^+ ions. The released amount of Ag from the aqueous solution (absorbance of 0.4 at 490 nm) of AgNCs/RB during the LED irradiation was evaluated by the ICP-MS. This evaluation revealed that the released Ag was 370 ppb, which is enough high concentration to show the antibacterial activity[17]. The Ag^+ ion release from AgNCs and the $^1O_2$ generation by RB can work as double antibacterial actions for dental a-PDT using the AgNCs/RB nanocomposite.

3.3 Antibacterial effects of AgNCs/RB and white LED on oral bacterial cells

The turbidity of oral bacterial cells was shown in Fig. 2. Application of AgNCs/RB and white LED irradiation were dose-dependently inhibited the growth of *S. mutans, P. gingivalis, and A. actinomycetemcomitans* (P<0.05). Especially, 10 μg/mL AgNCs/RB exhibited the significant reducing effect when compared to control (no application). The SEM images of *S. mutans* at 24 hr after incubation are shown in

Fig. 2B. In control (no application of AgNCs/RB), marked colonization of *S. mutans* was observed on the culture dish. In contrast, the sample received with AgNCs/RB (10 μg/mL) and white LED showed slight bacterial accumulation and less biofilm formation. In the assessment of LIVE/DEAD BacLight staining of *S. mutans*, control (no application of AgNCs/RB) was mostly stained in green, indicating live cells. When AgNCs/RB (10 μg/mL) and white LED were applied, *S. mutans* frequently stained red, indicating dead cells.

To compare the antibacterial activity of AgNCs/RB, AgNCs and RB, the amount of AgNCs and RB was adjusted to employ in culture test, as the mole ratio of 1:0.3 (AgNCs:RB). Fig. 3A and B show the turbidity of *S. mutans* and *A. actinomycetemcomitans*, respectively. When white LED irradiation was not applied, turbidity of *S. mutans* and *A. actinomycetemcomitans* was comparable in all groups. However, white LED irradiation with application of AgNCs/RB or RB significantly decreased the turbidity of bacterial cells when compared to control (no application). The combination of AgNCs/RB with white LED irradiation significantly inhibited the turbidity increase compared to AgNCs or RB. The LED irradiation to AgNCs/RB time-dependently decreased the turbidity of *S. mutans* (Fig. 3C). To assess the antibacterial effect of released Ag^+ ion, bacterial suspension was mixed into BHI

medium contained 10 μg/mL AgNCs/RB, after waiting 10, 60 and 900 sec since white LED irradiation. The turbidity of short wait time (10 sec) suppressed the turbidity of *S. mutans*, suggesting that Ag^+ ion released by oxidation of AgNCs exerted the antibacterial activity (Fig. 3D). However, long wait time (60 and 900 sec) did not show the reduction of turbidity.

3.4 Cytotoxic effects of AgNCs/RB on fibroblastic cells

The results of WST-8 and LDH activity assays are presented in Fig. 4A. WST-8 and LDH activity of fibroblastic cells were comparable in all groups after incubation for 24 hr. The LIVE/DEAD BacLight assay showed that cultured cells exhibited green fluorescence (live cells) in control (no application) and AgNCs/RB applied group (Fig. 4B). In addition, vinculin and F-actin associated with cell adhesion and spreading were detected, regardless of application of AgNCs/RB and white LED irradiation (Fig. 4B).

4. Discussion

The combination of AgNCs/RB with white LED significantly suppressed the growth of oral bacteria. These results were supported by SEM observation and

LIVE/DEAD staining, since photoexcited AgNCs/RB killed the bacterial cells and then reduced biofilm formation. As the result of fluorescence intensity measurement using MTX, photoexcited AgNCs/RB time-dependently generated $^1O_2$. Therefore, antibacterial effects of AgNCs/RB were mainly conducted by RB via $^1O_2$ generation. Oxidative stress by reactive oxygen species (ROS), such as $^1O_2$, superoxide, hydroxyl radical and hydrogen peroxide, may attack the unsaturated fatty acids in membrane and stimulate lipid peroxidation to form toxic substances such as aldehydes[21]. In addition, ROS interrupts the process of DNA replication[22] and promotes the degradation of amino acid of protein[23]. Further, application of AgNCs/RB and LED irradiation diminished the turbidity of periodontal pathogen bacteria; *A. actinomycetemcomitans* and *P. gingivalis*, suggesting antibacterial effect of photoexcited AgNCs/RB on periodontal bacteria. Since it was reported that $^1O_2$ was effective on Gram-negative and positive bacteria[24], a-PDT using AgNCs/RB may be beneficial as multitalented therapy in various dental treatments.

We hypothesized that $^1O_2$ generated by RB could also oxidize the AgNCs in the RB-conjugated AgNCs. In this study, photoexcited AgNCs/RB showed the absorbance decrease of AgNCs in the UV-vis spectrum, indicating the photodegradation of AgNCs to release Ag^+ ion. In fact, the released Ag was confirmed by ICP-MS. The antibacterial

PDT effects of AgNCs/RB against *S. mutans* and *A. actinomycetemcomitans* were greater than RB alone. Therefore, Ag-supply would up-regulate the inhibition of bacterial growth. Since activity of $^1O_2$ immediately disappear to be translated into $^3O_2$ [25], it was considered that antibacterial effect of $^1O_2$ was soon reduced after the LED off. However, Fig. 3D revealed that photoexcited AgNCs/RB exhibited the suppression of *S. mutans* growth in the condition of short waiting time. Therefore, it was speculated that released Ag^+ ion was remained in the long term in the BHI medium compared to $^1O_2$, to continuously exert the antibacterial activity. Our strategy, that is, a-PDT of both $^1O_2$ and Ag^+ ion as antimicrobial attacker of AgNCs/RB, was established. Previous report revealed that Ag^+ ion penetrated cell body and subjected the inhibition of DNA replication and inactivation of protein[26]. We also found the antimicrobial activity was disappeared in wait time of 60 and 900 sec. Supposedly, released Ag^+ ion bind other substances in the BHI medium to create the compound, due to its low ionization tendency. Ostermeyer et al.[27] reported that BSA, as a model protein, could absorb the Ag^+ ion released from AgNCs, to form chelate complex.

In general, antimicrobial materials frequently show cytotoxic adverse effects[26]. In the present study, the cell morphologies, WST-8 and LDH activity of mammalian cell were comparable in all groups, regardless of LED irradiation. Hence, this study revealed

AgNCs/RB possessed low cytotoxic effects on fibroblastic cells, even if generating of $^1O_2$ and Ag^+ ion. From the results of measurements of zeta potentials, charge of AgNCs/RB negatively sifted compared to AgNCs, suggesting that the stability of AgNCs/RB dispersion would be improved to enhance the biosafety. Dispersion degree of nanomaterial plays an important role in biocompatibility. Guo et al.[28] reported that well-dispersed nanomaterial, or carbon nanotubes, could improve their cytocompatibility in MTT assay. In addition, conventional dye; methylene blue, reportedly inhibited the cell proliferation at the concentration of clinical use for a-PDT use[29]. The advantages of AgNCs/RB include high cytocompatibility as well as great antimicrobial effects via $^1O_2$ generation and Ag^+ ion in comparison with conventional photosensitizer.

5. Conclusion

Photoexcited AgNCs/RB could generate $^1O_2$ and Ag^+ ion to exhibit the antibacterial effects. The combination of AgNCs/RB and white LED irradiation dose-dependently inhibited the growth of oral bacterial cells involving *S mutans, A actinomycetemcomitans and P gingivalis*, and significantly reduced the bacterial

turbidity compared to AgNCs or RB alone. Furthermore, application of AgNCs/RB in the absence of LED light showed low cytotoxicity against fibroblastic NIH3T3 cells. AgNCs/RB would be anticipated to be provided as the photosensitizer for dental a-PDT.

Acknowledgement

The authors acknowledge Prof. Hideya Kawasaki from the Chemistry and Materials Engineering, Faculty of Chemistry, Materials and Bioengineering, and Dr. Saori Miyata from the Department of Periodontology and Endodontology, Hokkaido University Faculty of Dental Medicine, for their technical and educational supports. This work was supported by JSPS KAKENHI (Grant Nos JP15H03520 and JP16K11822) and Tanaka Kikinzoku Memorial Foundation.

References

1) Wilson M : Lethal photosensitization of oral bacteria and its potential application in the photodynamic therapy of oral infections. Photochem Photobiol Sci 3 : 412-418, 2004.

2) Rajesh S, Koshi E, Philip K, Mohan A. Antimicrobial photodynamic therapy: An overview. J Indian Soc Periodontol 15 : 323-327, 2011.

3) Sivaramakrishnan G, Sridharan K : Photodynamic therapy for the treatment of peri-implant diseases: A network meta-analysis of randomized controlled trials. Photodiagnosis Photodyn Ther 21 : 1-9, 2018.

4) Soria-Lozano P, Gilaberte Y, Paz-Cristobal MP, Pérez-Artiaga L, Lampaya-Pérez V, Aporta J, Pérez-Laguna V, García-Luque I, Revillo MJ, and Rezusta A : In vitro effect photodynamic therapy with differents photosensitizers on cariogenic microorganisms. BMC Microbiol 15 : 187, 2015.

5) Parker S : The use of diffuse laser photonic energy and indocyanine green photosensitiser as an adjunct to periodontal therapy. BDJ 215 : 167-171, 2013.

6) Rosa LP, da Silva FC, Nader SA, Meira GA, Viana MS : Antimicrobial photodynamic inactivation of staphylococcus aureus biofilms in bone specimens using methylene blue, toluidine blue ortho and malachite green: An in vitro study. Arch Oral Biol 60 : 675-680, 2015.

7) Fotinos N, Convert M, Piffaretti JC, Gurny R, Lange N : Effects on gram-negative and gram-positive bacteria mediated by 5-aminolevulinic acid and 5-aminolevulinic acid derivatives. Antimicrob Agents Chemother 52 : 1366-1373, 2008.

8) Cieplik F, Tabenski L, Buchalla W, Maisch T : Antimicrobial photodynamic therapy for inactivation of biofilms formed by oral key pathogens. Front Microbiol 5 : 405, 2014.

9) Baier J, Maisch T, Maier M, Landthaler M, Baumler W : Direct detection of singlet oxygen generated by UVA irradiation in human cells and skin. J Invest Dermatol 127 : 1498-1506, 2007.

10) Bonnett, R : Photosensitizers of the porphyrin and phthalocyanine series for photodynamic therapy. Chem Soc Rev 24 : 19-33, 1995.

11) Zheng K, Setyawati MI, Leong DT, Xie J : Antibacterial Silver Nanomaterials. Coord Chem Rev 357 : 1-17, 2018.

12) Corrêa JM, Mori M, Sanches HL, da Cruz AD, Poiate E Jr, Poiate IA : Silver nanoparticles in dental biomaterials. Int J Biomater 2015: 485275, 2015.

13) Castillo JL, Rivera S, Aparicio T, Lazo R, Aw TC, Mancl LL, Milgrom P : The short-term effects of diammine silver fluoride on tooth sensitivity: a randomized controlled trial. J Dent Res 90 : 203-208, 2011.

14) Wang J, Li J, Guo G, Wang Q, Tang J, Zhao Y, Qin H, Wahafu T, Shen H, Liu X, Zhang X : Silvernanoparticles-modified biomaterial surface resistant to staphylococcus: new insight into the antimicrobial action of silver. Sci Rep 6 : 32699, 2016.

15) Roe D, Karandikar B, Bonn-Savage N, Gibbins B, Roullet JB : Antimicrobial surface functionalization of plastic catheters by silver nanoparticles. J Antimicrob Chemother 61 : 869-876, 2008.

16) Sangsuwan A, Kawasaki H, Matsumura Y, Iwasaki Y : Antibacterial silver nanoclusters bearing biocompatible phosphorylcholine-based zwitterionic protection. Bioconjug Chem 27 : 2527-2533, 2016.

17) Tominaga C, Shitomi K, Miyaji H, Kawasaki H : Antibacterial photocurable acrylic resin coating using a conjugate between silver nanoclusters and alkyl quaternary ammonium. ACS Appl Nano Mater 1 : 4809-4818, 2018.

18) Tominaga C, Hasegawa H, Yamashita K, Arakawa R, Kawasaki H : UV photo-mediated size-focusing synthesis of silver nanoclusters. RSC Adv 6 : 73600-73604, 2016.

19) Hirakawa K : Fluorometry of singlet oxygen generated via a photosensitized reaction using folic acid and methotrexate. Anal Bioanal Chem 393 : 999-1005, 2009.

20) Yamamoto M, Shitomi K, Miyata S, Miyaji H, Aota H, Kawasaki H : Bovine serum albumin-capped gold nanoclusters conjugating with methylene blue for efficient $^1O_2$ generation via energy transfer. J Colloid Interface Sci 510 : 221-227, 2018.

21) Birben E, Sahiner UM, Sackesen C, Erzurum S, Kalayci O : Oxidative stress and antioxidant defense. World Allergy Organ J 5 : 9-19, 2012.

22) Jena NR : DNA damage by reactive species: Mechanisms, mutation and repair. J Biosci 37 : 503-517, 2012.

23) Berlett BS, Stadtman ER : Protein oxidation in aging, disease, and oxidative stress. J Biol Chem 272 : 20313-20316, 1997.

24) Dahl TA, Midden WR, Hartman PE : Comparison of killing of gram-negative and gram-positive bacteria by pure singlet oxygen. J Bacteriol 171 : 2188-2194, 1989.

25) Moan J, Berg K : The photodegradation of porphyrins in cells can be used to estimate the lifetime of singlet oxygen. Photochem Photobiol 53 : 549-553, 1991.

26) Rizzelloa L, Pompa PP : Nanosilver-based antibacterial drugs and devices: Mechanisms, methodological drawbacks, and guidelines. Chem Soc Rev 43 : 1501-1518, 2014.

27) Ostermeyer AK, Mumuper CK, Semprini L, Radniecki T : Influence of bovine serum albumin and alginate on silver nanoparticle dissolution and toxicity to nitrosomonas europaea. Environ Sci Technol 47 : 14403-14410, 2013.

28) Guo YK, Chen W, Xiong Q, Ren QX, Sun L, Han B, Li XJ : Chemically modified multiwalled carbon nanotubes improve the cytocompatibility. Mater Res Express 4 : 125801, 2017.

29) Miyata S, Miyaji H, Kawasaki H, Yamamoto M, Nishida E, Takita H, Akasaka T, Ushijima N, Iwanaga T, Sugaya T : Antimicrobial photodynamic activity and cytocompatibility of $Au_{25}(Capt)_{18}$ clusters photoexcited by blue LED light irradiation. Int J Nanomedicine 12 : 2703-2716, 2017.

Fig. 1

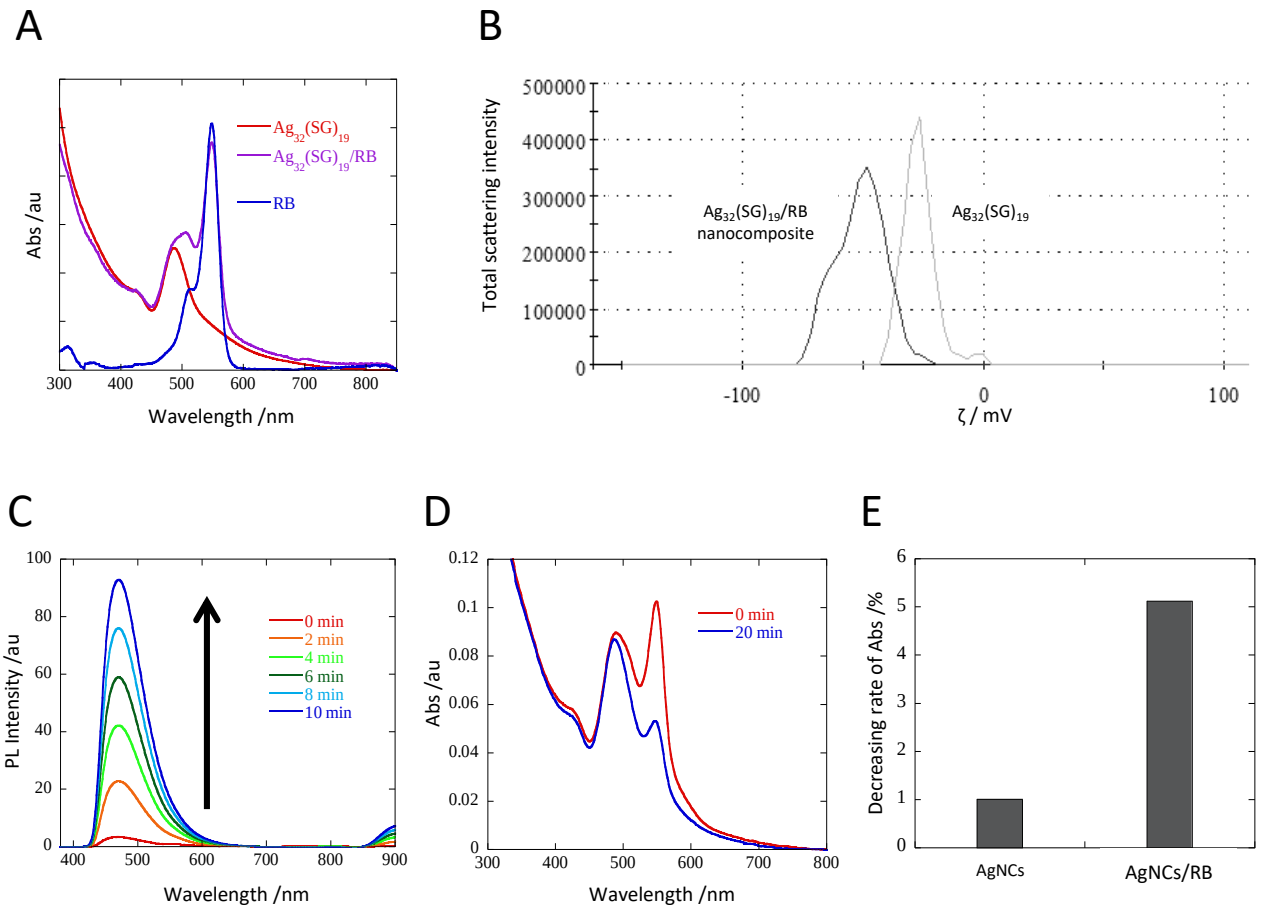
A
Abs /au
Wavelength /nm
$Ag_{32}(SG)_{19}$
$Ag_{32}(SG)_{19}$/RB
RB
B
Total scattering intensity
$Ag_{32}(SG)_{19}$/RB nanocomposite
$Ag_{32}(SG)_{19}$
ζ / mV
C
PL Intensity /au
Wavelength /nm
0 min
2 min
4 min
6 min
8 min
10 min
D
Abs /au
Wavelength /nm
0 min
20 min
E
Decreasing rate of Abs /%
AgNCs
AgNCs/RB

Fig. 2

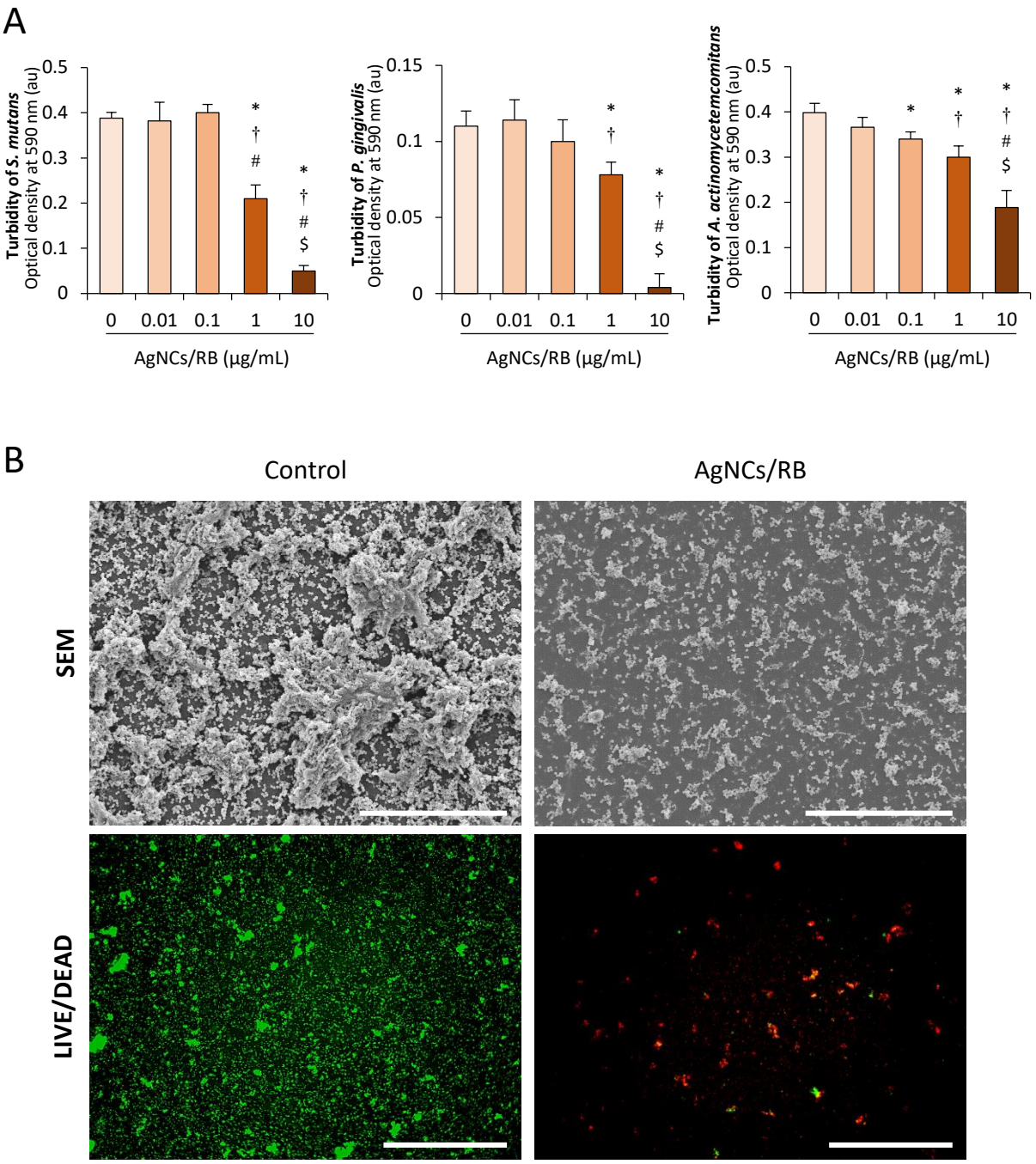
A
Turbidity of S. mutans
Optical density at 590 nm (au)
0.5
0.4
0.3
0.2
0.1
0
0
0.01
0.1
1
10
AgNCs/RB (μg/mL)
Turbidity of P. gingivalis
Optical density at 590 nm (au)
0.15
0.1
0.05
0
Turbidity of A. actinomycetemcomitans
Optical density at 590 nm (au)
B
Control
AgNCs/RB
SEM
LIVE/DEAD

Fig. 3

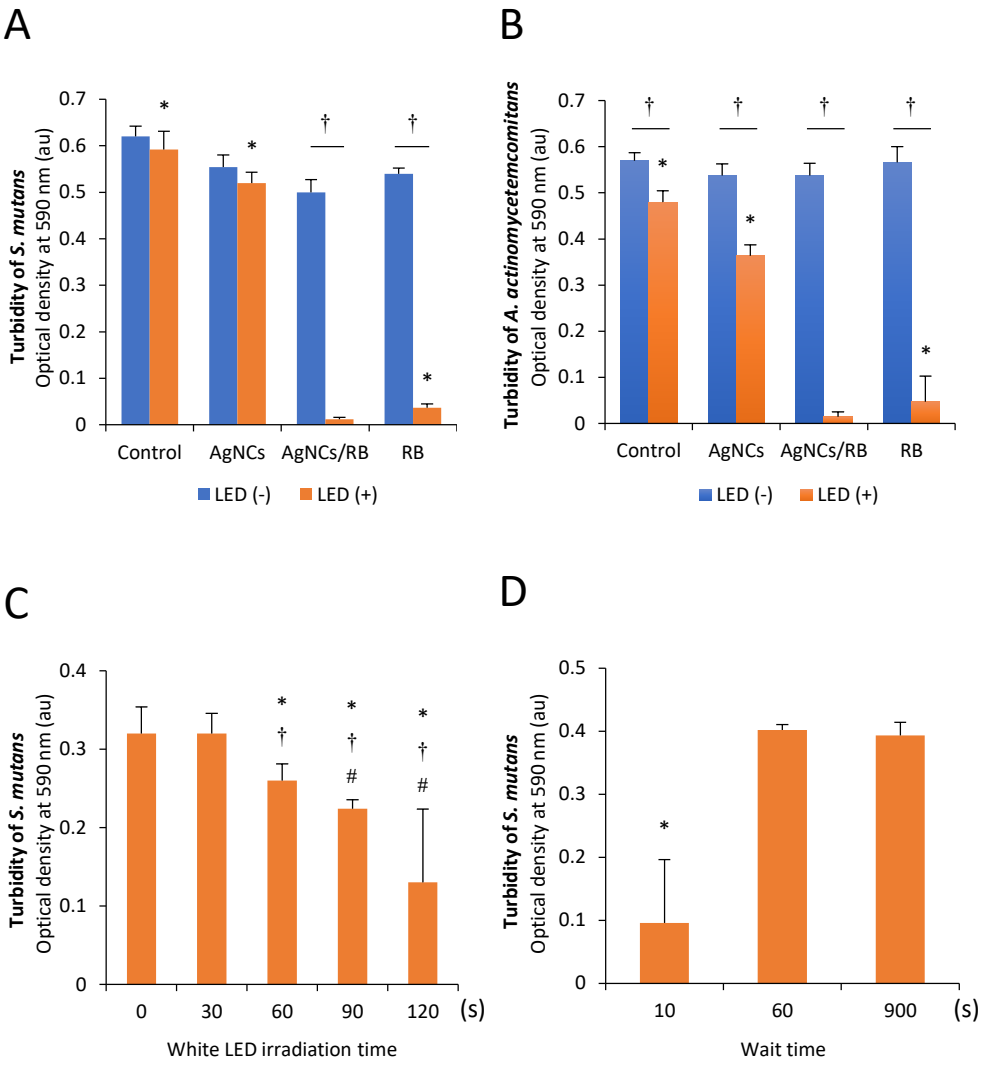
A
Turbidity of S. mutans
Optical density at 590 nm (au)
0.7
0.6
0.5
0.4
0.3
0.2
0.1
0
Control
AgNCs
AgNCs/RB
RB
LED (-)
LED (+)
B
Turbidity of A. actinomycetemcomitans
Optical density at 590 nm (au)
Control
AgNCs
AgNCs/RB
RB
LED (-)
LED (+)
C
Turbidity of S. mutans
Optical density at 590 nm (au)
0.4
0.3
0.2
0.1
0
0
30
60
90
120
(s)
White LED irradiation time
D
Turbidity of S. mutans
Optical density at 590 nm (au)
0.5
0.4
0.3
0.2
0.1
0
10
60
900
(s)
Wait time

Fig. 4

A

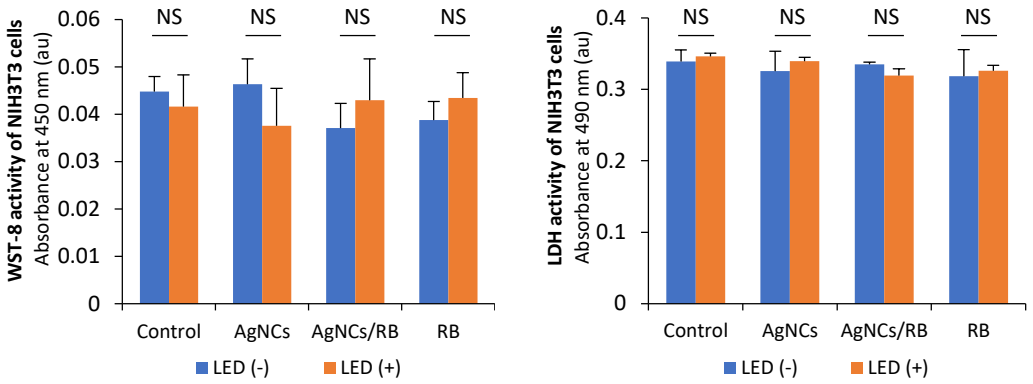
WST-8 activity of NIH3T3 cells
Absorbance at 450 nm (au)
0.06
0.05
0.04
0.03
0.02
0.01
0
NS
NS
NS
NS
Control
AgNCs
AgNCs/RB
RB
LED (-)
LED (+)
LDH activity of NIH3T3 cells
Absorbance at 490 nm (au)
0.4
0.3
0.2
0.1
0
NS
NS
NS
NS
Control
AgNCs
AgNCs/RB
RB
LED (-)
LED (+)

B

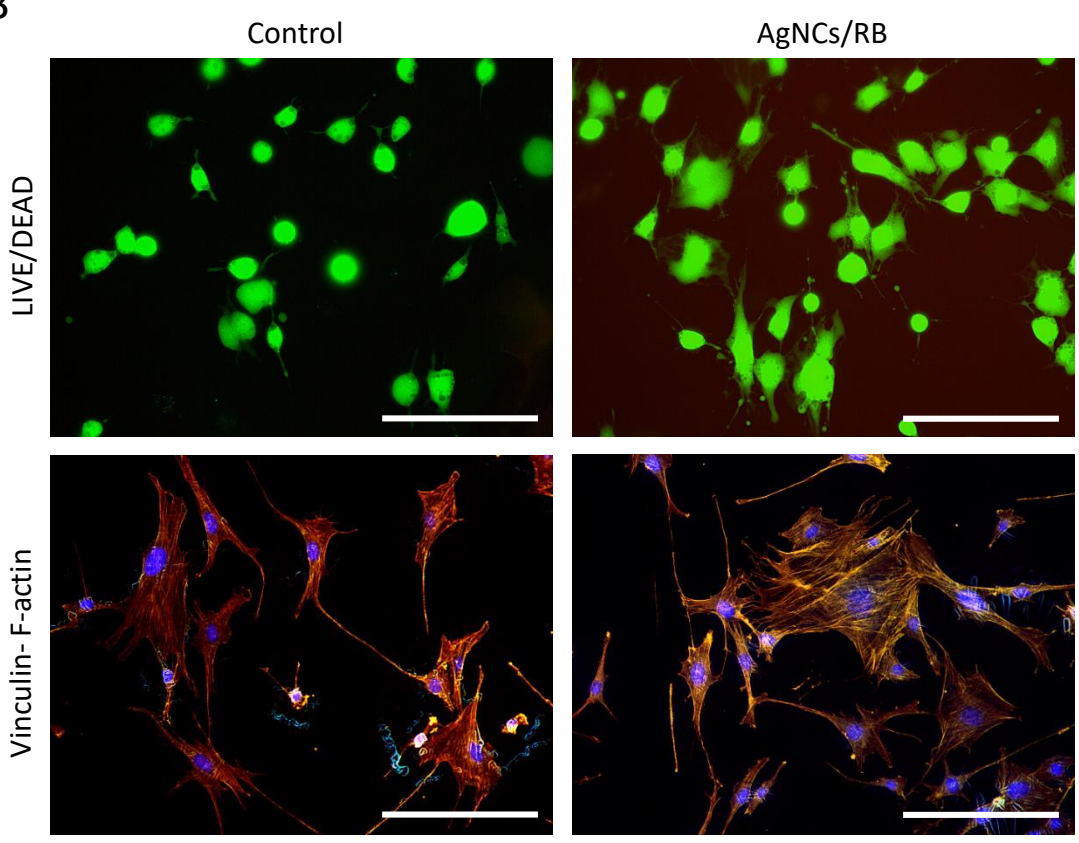
Control
AgNCs/RB
LIVE/DEAD
Vinculin- F-actin

Figure legends

Fig. 1. Characterization of AgNCs/RB

(A) The UV-vis spectra of AgNCs (red line), the AgNCs/RB nanocomposite (purple line) and RB (blue line). (B) The zeta potential of AgNCs and AgNCs/RB. (C) Fluorescence spectra of a MTX-containing solution of AgNCs/RB. (D) The UV-vis spectra of AgNCs/RB nanocomposite before (red line) and after the white LED irradiation (blue line). (E) Decreasing ratio of absorbance when irradiated with white LED of AgNCs and AgNCs/RB.

Abbreviations: Abs, Absorbance; AgNCs, Ag nanoclusters; au, arbitrary unit; LED, light-emitting diode; MTX, methotrexate; PL, photoluminescence. RB, rose bengal; UV, ultra violet.

Fig. 2. Evaluation of antibacterial activity of AgNCs/RB

(A) Antimicrobial effects of AgNCs/RB on oral bacterial cells after 24hr incubation (n=5, mean ± SD). Turbidity of *S. mutans*, *P. gingivalis and A. actinomycetemcomitans*: *, $P<0.05$ vs. 0 μg/mL AgNCs/RB; †, $P<0.05$ vs. 0.01 μg/mL AgNCs/RB; #, $P<0.05$ vs. 0.1 μg/mL AgNCs/RB; and $, $P<0.05$ vs. 1 μg/mL AgNCs/RB. (B) SEM observation

and LIVE/DEAD BacLight staining of *S. mutans* after incubation for 24 hr in control and AgNCs/RB groups. Scale bar represents 50 μm.

Abbreviations: AgNCs, Ag nanoclusters; LED, light-emitting diode; RB, rose bengal; SD, standard deviation; SEM, scanning electron microscopy; *A. actinomycetemcomitans, Aggregatibacter actinomycetemcomitans*; *P. gingivalis, Porphyromonas gingivalis*; *S. mutans, Streptococcus mutans.*

Fig. 3. Antibacterial characterization of AgNCs/RB

(A-B) The turbidity of control (no application), AgNCs, RB, and AgNCs/RB groups of *S. mutans* (n=5, mean ± SD) (A) and *A. actinomycetemcomitans* (n=4, mean ± SD) (B). *, $P<0.05$ vs. AgNCs/RB with LED (+); †, $P<0.05$. (C) Turbidity of *S. mutans* related to white LED irradiation time (0, 30, 60, 90 and 120 sec) (n=5, mean ± SD). *, $P<0.05$ vs. 0 s; †, $P<0.05$ vs. LED irradiated for 30 sec; and #, $P<0.05$ vs. LED irradiated 60 sec. (D) Turbidity of *S. mutans* in AgNCs/RB-contained medium. Bacterial suspension was mixed into the medium after waiting 10, 60 and 900 sec after LED irradiation (n=5, mean ± SD). *, $P<0.05$ vs. 60 and 900 sec.

Abbreviations: AgNCs, Ag nanoclusters; LED, light-emitting diode; RB, rose bengal; SD, standard deviation; *A. actinomycetemcomitans, Aggregatibacter actinomycetemcomitans*; *S. mutans, Streptococcus mutans.*

Fig. 4. Assessments of cytotoxic effect of AgNCs/RB

(A) WST-8 and LDH activities of NIH3T3 cells in control (no application), AgNCs, RB, and AgNCs/RB groups (n=6, mean ± SD). (B) LIVE/DEAD BacLight staining and vinculin-F-actin double staining of NIH3T3 cells after 24 hr incubation in control and AgNCs/RB groups. Scale bar represents 50 μm.

Abbreviations: AgNCs, Ag nanoclusters; au, arbitrary unit; LDH, lactate dehydrogenase; LED, light-emitting diode; NS, Not significant; RB, rose bengal; SD, standard deviation; WST, water-soluble tetrazolium salt.